Study on hyperspectral estimation model of soil organic carbon content in the wheat field under different water treatments

Chenbo Yang
Shanxi Agricultural University
Meichen Feng (fmc101@163.com)
Shanxi Agricultural University
Lifang Song
Shanxi Agricultural University
Chao Wang
Shanxi Agricultural University
Wude Yang
Shanxi Agricultural University
Yongkai Xie
Taiyuan Normal University
Binghan Jing
Shanxi Agricultural University
Lujie Xiao
Shanxi Agricultural University
Meijun Zhang
Shanxi Agricultural University
Xiaoyan Song
Shanxi Agricultural University
Muhammad Saleem
Shanxi Agricultural University

Research Article

Keywords: SOC, hyperspectral PLSR mathematical transformation sample allocation ratio

Posted Date: May 18th, 2021

DOI: https://doi.org/10.21203/rs.3.rs-530273/v1

Study on hyperspectral estimation model of soil organic carbon content in the wheat field under different water treatments

Chenbo Yang[1], Meichen Feng[1*], Lifang Song[1], Chao Wang[1], Wude Yang[1], Yongkai Xie[2], Binghan Jing[1], Lujie Xiao[1], Meijun Zhang[1], Xiaoyan Song[1], Muhammad Saleem[1]

[1]*Agronomy college, Shanxi Agricultural University, 030801, Taigu, Shanxi, China*

[2] *Institute of Geography Science, Taiyuan Normal University, 030619, Jinzhong, Shanxi, China*

Abstract: Hyperspectral remote sensing technology can realize the rapid, real-time, and non-destructive monitoring of soil nutrient changes, which is of great significance to promote the development of precision agriculture. In this paper, 225 soil samples were taken as the research object to study the influence of different water treatment on soil organic carbon content, and the relationship between soil organic carbon content and spectral reflectance. After spectral preprocessing, the hyperspectral monitoring models of SOC content were constructed by partial least squares regression(PLSR) with five different sample allocation ratios of calibration to validation sets. The results showed that the effects of drought stress on SOC content were different in different growth stages of winter wheat. Results of correlation analysis showed that the differential transformation can refine the spectral characteristics and improve the correlation between SOC content and spectral reflectance. Results of model construction showed that the models constructed by second-order differential transformation were not effective, but the RPD values of the models were constructed by simple mathematical transformation(T0-T5) and first-order differential transformation(T6-T11) can reach more than 1.4. The simple mathematical transformation(T0-T2, T4-T5) and the first-order differential transformation(T6-T10) resulted in the highest RPD in mode 5 and mode 2, respectively. Among all the models, the model of T7 in

*Corresponding author: Meichen Feng. E-mail: fmc101@163.com

mode 2 reach the highest accuracy with a RPD value of 1.9861. Therefore, it is necessary to consider the data preprocessing algorithm and allocation ratio in the construction of SOC hyperspectral monitoring model.

Key words: SOC, hyperspectral, PLSR, mathematical transformation, sample allocation ratio

1. Introduction

Soil organic matter is the material derived from living organisms in the soil, of which 60-80% of the carbon component is called soil organic carbon(SOC). It is well known that SOC is a vital factor to improve soil fertility, although the content is small [1-3]. However, the previous methods to obtain soil organic carbon content are time-consuming and laborious. Hyperspectral technology can solve this problem. In recent years, with the development of hyperspectral remote sensing technology, due to its characteristics of rapid, real-time, and non-destructive monitoring of targets [4], it has been become an important technology for many scholars to study the soil properties [5-7].

The spectral reflectance refers to the ratio of reflected flux to the incident flux at a certain wavelength [8]. Various molecules in the soil absorb and reflect light at different wavelengths to form soil characteristic curve, the visible(350-780 nm) and near-infrared(780-2500 nm) bands have been widely used in agricultural research [9-10]. In the process of quantitative analysis of chemical measurement values and hyperspectral data, analysis result is mainly affected by three aspects: the expression ability of hyperspectral data [11-16], the data reasonable allocation of calibration to validation sets [17], and the scientific selection of model construction method [18-22]. The expression ability of hyperspectral data refers to reducing the noise of original spectral data through different spectral transformation algorithms, and improving the correlation between the spectral data and the chemical measurement values [23-24]. The data reasonable allocation of

45 calibration to verification sets will be affected by the amount of data and the degree of dispersion,
46 which is also a segment that is easy to be ignored in the process of model construction [25]. The
47 scientific selection of the model construction method is determined by the quantitative relationship
48 between the chemical measurement values and the spectral data. At present, there are many kinds
49 of methods to construct model using soil property data and corresponding spectral data. Some
50 simple linear models include stepwise multiple linear regression(SMLR), partial least squares
51 regression(PLSR), and principal component regression(PCR), etc. Nonlinear models include
52 artificial neural network(ANN), support vector machine(SVM), and random forests(RF) [26-28], etc.
53 PLSR is a kind of linear regression model which has been widely used and has a good effect [29-32].
54 Previous studies have shown that hyperspectral monitoring has a good ability to predict SOC
55 content [33-34]. PLSR was used in many studies on the hyperspectral monitoring model of SOC
56 content, but the results were different. Amin et al.[35] constructed a hyperspectral monitoring model
57 of SOC content based on PLSR in Azerbaijan, and found that the model constructed after
58 Savitzky-Golay smoothing can reach the highest accuracy with R^2 and RPD are 0.85 and 2.54,
59 respectively. Yu et al.[36] constructed a hyperspectral monitoring model of soil organic matter
60 content by PLSR through different preprocessing of spectral data, and the results showed that the
61 model constructed by continuous removal (CR) had the best accuracy. Ji et al.[17] used a variety of
62 modeling methods to predict soil organic matter content based on different data allocation ratios, it
63 was found that when the ratios of calibration to validation sets were different, the accuracy of
64 model constructed by different methods was different. But the data allocation ratios used in this
65 study were few, and hyperspectral data were not preprocessed.
66 According to previous studies, different data preprocessing algorithm, data allocation ratio,

and modeling method all have an effect on the accuracy of the model. In this paper, from the perspective of the data allocation ratio, different mathematical transformations of spectral data were carried out, and the PLSR was used to construct the model. The purposes of this study are: (1) Study the effect of mathematical transformation algorithm and data allocation ratio on the construction of hyperspectral monitoring model of SOC content, (2) Find the best spectral preprocessing algorithm and data allocation ratio to predict SOC content.

2. Materials and methods

2.1 Experimental design

The experimental field located in the Experiment Station of Shanxi Agricultural University. Each experimental plot is all a square of 9 m^2, with a total of 15 plots. The water content was controlled according to the percentage of the maximum soil field capacity. There were five irrigation levels: 80%, 60%, 45%, 35%, and 30%. The experiment was set up in a completely randomized design with three replications. The winter wheat cultivar 'Zhongmai 175' was planted, and the soil drill was used to collect topsoil of 0-20 cm in each critical growth period of winter wheat. The experiment was carried out for two years, sampling 8 times and 7 times in 2018 and 2019, respectively. The soil texture for the experimental field is calcareous cinnamon soil developed from loess parent material with medium fertility, the average total nitrogen content, the total phosphorus content, and the total potassium content are 0.70 $g \cdot kg^{-1}$, 1.32 $g \cdot kg^{-1}$, and 22.13 $g \cdot kg^{-1}$, respectively.

2.2 Indexes measurement

Before the measurement, the animal, plant residues, and other impurities were removed from samples. After drying in the shade, passed through a 0.154 mm sieve. Then measured soil spectral

reflectance and SOC content.

2.2.1 Soil reflectance measurement

The Field-spec 3 hyperspectral radiometer produced by ASD company in the United States was used for soil spectral measurement, and the wavelength acquisition range is 350-2500 nm. Before the measurement, each soil sample with a flat surface was placed in a culture dish. The probe was placed at about 1 mm above the soil surface and kept perpendicular. Three points were measured for each sample, and each point was measured 10 times. Before each measurement, the whiteboard was used for calibrating.

2.2.2 SOC content measurement

SOC content was measured by the Walkley–black method [29].

2.3 Data processing and analysis

There being 17 common mathematical algorithms were selected to preprocessing the original spectral data of soil, as it showed in Table 1.

Table 1 Soil spectral preprocessing mathematical algorithms

Simple mathematical transformation		**First-order differential transformation**		**Second-order differential transformation**	
code	algorithm	**code**	algorithm	**code**	algorithm
T0	*R*	**T6**	*R'*	**T12**	*R"*
T1	*1/R*	**T7**	*(1/R)'*	**T13**	*(1/R)"*
T2	*Log R*	**T8**	*(Log R)'*	**T14**	*(Log R)"*
T3	*1/Log R*	**T9**	*(1/Log R)'*	**T15**	*(1/Log R)"*
T4	$\sqrt{R}$	**T10**	$(\sqrt{R})'$	**T16**	$(\sqrt{R})"$
T5	$1/\sqrt{R}$	**T11**	$(1/\sqrt{R})'$	**T17**	$(1/\sqrt{R})"$

Note: R represents the original spectrum

In this paper, 225 samples were divided into calibration set and verification set by concentration gradient method [37], including 5 samples allocation ratios(calibration set: verification set): mode 1(2:2), mode 2(3:2), mode 3(4:2), mode 4(5:2), mode 5(6:2).

In this paper, PLSR models were constructed in MATLAB 2010, and leave one out

cross-validation method was selected to improve the stability of the model. The coefficient of determination (R^2), root mean square error (RMSE), and the ratio of standard deviation to the standard prediction error (RPD) were used to evaluate the accuracy of the model.

This paper also uses View Spec Pro 6.0 to preprocess soil spectral data, Excel 2010, Unscrambler 9.7, and SPSS 20 for data processing, Origin 2016 for mapping.

3. Results and analysis

3.1 Change of SOC content

It can be seen from Fig.1 that the change trends of SOC content are different with the advance of the winter wheat growth process in the two-year experiment. In 2018, there is an obvious increase-decrease-increase trend, while in 2019 is slowly decreasing to a stable trend. We compare the sampling stages that have close days after sowing in two-year. 160 days and 203 days after sowing in 2018 correspond to 164 days and 203 days after sowing in 2019, respectively. SOC content increased first and then decreased with the aggravation of drought stress, but their significance of difference was different. Although the change trends of 188 days and 194 days after sowing in 2018 and 191 days after sowing in 2019 were different, there was no significant difference in SOC content among the three growth stages. SOC content in 209 days, 224 days, 232 days, and 242 days after sowing in 2018 basically decreased with the aggravation of drought stress, while the change trends of 211 days, 218 days, 228 days, and 236 days after sowing in 2019 were opposite.

3.2 Descriptive statistical analysis

225 samples were analyzed in this paper, it can be seen from Table 2 that the standard deviation of the SOC content was small. The samples have a certain negative skewness, and the

data distribution trend was slower than the standard normal distribution, but basically conformed to the normal distribution. In different allocation modes, the minimum and maximum values of the total data set were all assigned to the calibration sets. The average value and standard deviation of the calibration sets and the verification sets were close, this means that the data dispersion was similar. At the same time, the calibration sets and verification sets in the five modes all basically conformed to normal distribution, which can be used for subsequent processing.

Table 2 Descriptive statistical analysis of test samples

	Num	Min ($g \cdot kg^{-1}$)	Max ($g \cdot kg^{-1}$)	Ave	SD	Skewness	Kurtosis
Total	225	4.296	13.013	9.226	1.678	-0.288	-0.098
Cal-set of Mode 1	113	4.296	13.013	9.222	1.702	-0.314	-0.008
Ver-set of Mode 1	112	4.631	13.009	9.230	1.661	-0.263	-0.151
Cal-set of Mode 2	135	4.296	13.013	9.227	1.682	-0.295	-0.065
Ver-set of Mode 2	90	4.632	13.009	9.225	1.682	-0.283	-0.085
Cal-set of Mode 3	150	4.296	13.013	9.226	1.678	-0.287	-0.096
Ver-set of Mode 3	75	4.632	13.009	9.227	1.690	-0.296	-0.026
Cal-set of Mode 4	161	4.296	13.013	9.232	1.688	-0.291	-0.046
Ver-set of Mode 4	64	5.041	12.721	9.211	1.666	-0.290	-0.156
Cal-set of Mode 5	169	4.296	13.013	9.224	1.691	-0.301	-0.040
Ver-set of Mode 5	56	5.041	12.829	9.232	1.655	-0.253	-0.209

Note: Num, Min, Max, Ave, SD, Cal-set, and Ver-set are number, minimum, maximum, average, standard deviation of samples, calibration set, and verification set, respectively.

3.3 Changes of original spectral reflectance

Since 93% of the 225 samples used in this paper were concentrated in the middle of 6-12

141 $g \cdot kg^{-1}$, it was necessary to analyse the soil spectral reflectance variation of SOC content at
142 different levels(6, 7, 8, 9, 10, 11 $g \cdot kg^{-1}$). It can be seen from Fig.2 that the changing trends of soil
143 spectral reflectance with different SOC content levels were basically consistent. The reflectance
144 increases with the increase of wavelength, and obvious absorption valleys were formed at near
145 1400 nm, 1900 nm, and 2200 nm. With the increase of SOC content, soil spectral reflectance
146 decreased gradually, but the change range was uneven. The spectral curves of two samples with
147 the SOC content of 6 and 7 $g \cdot kg^{-1}$ were close, and those of 8, 9, and 10 $g \cdot kg^{-1}$ were close to each
148 other.

149 3.4 Changes of preprocessing spectral reflectance

150 In this paper, one sample(SOC content is 9.222 $g \cdot kg^{-1}$) with the closest average content
151 among all samples was taken as an example, and spectral preprocessing was performed according
152 to Table 1. Fig.3 showed that compared with the original spectral curve(T0), different
153 preprocessing algorithms have different influences. Except for T2 and T4, the changing trends of
154 other spectral preprocessing curves all had an obvious change. Among different types of
155 preprocessing algorithms, the first-order differential transformation and the second-order
156 differential transformation have an obvious effect on refining spectral characteristics.

157 3.5 Correlation analysis between SOC content and different preprocessing spectrum

158 It can be seen from Fig.4 that the correlations between SOC content and the spectral
159 reflectance of T0-T5 were between ±0.15, while the correlations of T6-T17 were improved.
160 Among them, the correlations of T12-T17 after second-order differential transformation were
161 basically within ±0.4, and that of T6-T11 after first-order differential transformation were within
162 ±0.6. In addition, the correlations of T6 and T10 in some wave bands can reach ±0.7 to ±0.8.

Although differential transformation can improve the correlation between the spectral reflectance and SOC content, the second-order differential transformation has a slight improvement only, however, the first-order differential transformation can improve the correlation greatly. The result showed that the differential transformation may enlarge the spectral characteristics of some wave bands which have a great correlation with SOC content, and the effect of first-order differential transformation was better than second-order differential transformation.

3.6 Construction and validation of PLSR model

Fig.5 showed that the accuracy of the models constructed by the first-order differential transformation, compared with the simple mathematical transformation, was increased, but the accuracy of the models constructed by the second-order differential transformation was reduced. Among all the models, the accuracy and stability of T6-T8 and T10-T11 after first-order differential transformation were basically reached the highest in mode 3, and T9 in mode 5 was also higher.

Fig.6 showed that the validation accuracy of the models constructed by the second-order differential transformation was low in all modes. Combined with Fig.5, it can be seen that the second-order differential transformation was not conducive to the construction of PLSR hyperspectral monitoring model for SOC content. The models constructed by simple mathematical transformation and first-order differential transformation achieved the highest verification accuracy in mode 5 and mode 2, respectively. At the same time, the verification accuracy of each model constructed by first-order differential transformation was higher than that of the corresponding simple mathematical transformation. Combined with Fig.5, it can be seen that the accuracy of PLSR hyperspectral monitoring models for SOC content can be improved by

first-order differential transformation for soil spectral data. Different from Fig.5, the accuracy of the models constructed by simple mathematical transformation and first-order differential transformation reached the lowest in mode 3. It can be seen that it is necessary to consider the different sample allocation ratio of calibration to verification sets while performing a mathematical transformation on hyperspectral data to improve the model accuracy. Among all the models constructed in this study, T7 and T11 reached the highest accuracy in mode 2 and mode 5, RPD are 1.9861 and 1.9217, respectively.

4. Discussion

The quantitative analysis of soil property data and hyperspectral data to achieve real-time and non-destructive monitoring model data is an important direction of soil research in recent years. SOC content is one of the common research property [38-40]. In this paper, based on 225 soil data, 17 mathematical transformation algorithms, 5 different data allocation ratios of the calibration to validation sets, and PLSR was selected for constructing the hyperspectral monitoring model of SOC content. The goal is going to select the best spectral preprocessing mathematical algorithm and the optimal data allocation ratio of calibration to validation sets for hyperspectral monitoring of SOC content.

From Fig.1, we can see that the change trends of SOC content with the advance of the winter wheat growth process are different in the two-year experiment, and the change trend of SOC content show an opposite trend with the aggravation of drought stress appears in the later stage of the experiment. This may be due to the different climatic conditions lead to the difference in the growth of winter wheat in the two-year experiment. In fact, the growth of winter wheat in the second year was not as good as that in the first year. Severe high temperature and drought weather

207 occurred in the experimental plot from March to April of 2019. During this period, the winter
208 wheat is in the stage from turning green to jointing, and the water demand is high. The high
209 temperature leads to water shortage of crops and affects the later growth [41]. In May 2019, the
210 temperature of the experimental site fluctuated greatly, frost disaster occurred in the early stage,
211 and high temperature above 35 ℃ appeared in the later stage. The extreme temperature further
212 affected the growth of winter wheat [42].

213 In this paper, the change of the spectral reflectance of soil with different SOC content have
214 been compared. It was found that the spectral reflectance of soil with different SOC content
215 increased gradually with the increase of wavelength, and obvious absorption valleys were formed
216 near 1400 nm, 1900nm and 2200nm. Physical studies show that the spectrum in the visible region
217 is caused by the outer electron transition, while the near-infrared spectrum is mainly affected by
218 molecular vibration, which can reflect the composition and structure of molecules. This is the
219 basic principle of quantitative analysis of target materials by using hyperspectral spectroscopy. It
220 ensures that almost no two substances have the same spectral characteristics, but also ensures that
221 the same kind of substances have certain similar spectral characteristics [43]. These absorption
222 valleys are caused by water molecules, OH^- and minerals [44]. At the same time, it was also found
223 that the overall value of soil spectral reflectance will decrease with the increase of SOC content,
224 which was consistent with the previous research results [45]. This may be due to the higher content
225 of organic carbon molecules absorbed more light, which may also be one of the principles of
226 quantitative monitoring SOC content with hyperspectral.

227 Compared with the original spectral data (T0), simple mathematical transformation such as
228 T1-T5 simply changed the change trend or value of the spectral curve, which is caused by the

mathematical properties of these simple transformation algorithms. The curves after the first-order differential transformation (T6-T11) and the second-order differential transformation (T12-T17) have changed greatly. According to the mathematical characteristics of the first-order differential and the second-order differential, they can magnify the increase, decrease, concavity and convexity at some wavelengths that are difficult to be recognized by the naked eye. Therefore, the differential transformation plays an obvious role in refining the spectral information [46-47].

In terms of improving the correlation between SOC content and spectral data, simple mathematical transformation(T1-T5) did not significantly improve compared with T0. T2 and T4 were basically the same as T0, while T1, T3, and T5 only changed the positive and negative correlation at the some wavelengths. The first-order and second-order differential transformation improved the correlation between spectral reflectance and SOC content in varying degrees, and the effect of first-order differential transformation was better than second-order differential transformation. At the same time, the results of model construction showed that the RPD value of the models constructed by simple mathematical transformation and first-order differential transformation reached more than 1.4, which were higher than that of the second-order differential transformation. It can be seen, from the mathematical characteristics of the first-order differential, that the characteristic spectrum of SOC content is not only limited to some individual wavelengths, but also related to the increase and decrease of some continuous wave bands. At the same time, it is necessary to properly preprocess the spectral data before constructing the hyperspectral monitoring model.

Extracting sensitive band or using full band is a common way to construct hyperspectral quantitative monitoring model of SOC content. Some studies have shown that 435 nm, 500 nm,

965 nm, 1409 nm, 1910 nm, 2170 nm, 2260 nm and 2380 nm are sensitive bands of SOC [44, 48]. Although the model constructed by using sensitive bands can be more concise and efficient, it can be seen from Fig.4 that the spectral characteristics of soil organic carbon content may also be related to the change trend of spectral curve. In this case, it is necessary to consider using the full band. PLSR can effectively deal with the complex relationship of high-dimensional data and provide a quantitative model. Therefore, this paper uses PLSR as the model building method.

In this paper, it was found that the R^2_{cv} of the models constructed by the second-order differential transformation were mostly below 0.6, and $RMSE_{cv}$ were higher, the accuracy of model construction was lower than that of simple mathematical transformation and first-order differential transformation. At the same time, the model validation results also showed that the accuracy of models constructed by second-order differential transformation was lower than that of simple mathematical transformation and first-order differential transformation, except for individual models. The accuracy of the models with different sample allocation ratios was different under the same mathematical transformation. In addition to T3 and T11 reached the highest RPD in mode 1 and mode 5, respectively. Other simple mathematical transformation and first-order differential transformation reached the highest RPD in mode 5 and mode 2, respectively. Generally speaking, among the different mathematical transformation algorithms, the models constructed by the first-order differential transformation have the best effect. The model construction and verification accuracy was the best in mode 3 and mode 2, and reached the highest in T10 and T7, respectively.

In this study, R^2_{cv} and $RMSE_{cv}$ were obtained by cross-validation that were used as the indicators to evaluate the accuracy of model construction. Therefore, with the increase of the

number of samples in the calibration set, the more time it takes and the higher the requirement for a computer to construct the model using PLSR. In practice, mode 2 can save more time and computer memory. Therefore, in the process of constructing a hyperspectral monitoring model of SOC content, the first-order differential transformation combined with a sample allocation ratio of 3:2 (calibration set: validation set) is conducive to improve the model accuracy and stability.

5. Conclusion

The prediction accuracy of the hyperspectral monitoring model of SOC content is greatly affected by soil spectral preprocessing mathematical algorithms and the ratio of the calibration set to validation set. Different mathematical transformation preprocessing can enlarge or reduce some characteristic information of the original spectral data. Reasonable data allocation ratio can reduce the excessive redundancy of calibration set. But different mathematical transformation algorithms have different requirements for the ratio of the calibration set to verification set. Therefore, in order to improve the accuracy of the model, it is necessary to comprehensively consider the mathematical transformation algorithm and sample allocation ratio.

This study showed that the effects of drought stress on soil organic carbon content were different in different growth stages of winter wheat, and the higher the SOC content, the lower the spectral reflectance. The first-order differential transformation and the second-order differential transformation have a greater role in amplifying spectral information, and can also significantly improve the correlation between SOC content and spectral reflectance, the maximum correlation can reach ±0.8. The prediction accuracy of the hyperspectral monitoring model of SOC content can be effectively improved by first-order differential transformation and the sample allocation ratio of calibration set: verification set = 3:2. Among them, the model constructed by the first

reciprocal transformation and then the first-order differential transformation has the highest accuracy, and the RPD of the verification model is 1.9861.

Reference

1. Aryal, D.R., De Jong, B.H., Ochoa-Gaona, S., Esparza-Olguin, L. & Mendoza-Vega, J. Carbon stocks and changes in tropical secondary forests of southern Mexico. *Agr Ecosyst Environ*. **195**, 220-230(2014).
2. Aryal, D.R., De Jong, B.H., Ochoa-Gaona, S., Mendoza-Vega, J. & Esparza-Olguin, L. Successional and seasonal variation in litterfall and associated nutrient transfer in semi-evergreen tropical forests of SE Mexico. *Nutr Cycl Agroecosys*. **103**(1), 45-60(2015).
3. Aryal, D.R. *et al*. Soil organic carbon depletion from forests to grasslands conversion in Mexico: A review. *Tropical Agriculture*. **8**, 181(2018).
4. Qi, H., Paz-Kagan, T., Karnieli, A., Jin, X. & Li, S. Evaluating calibration methods for predicting soil available nutrients using hyperspectral VNIR data. *Soil Till Res*. **175**, 267-275(2018).
5. Dong, X., Tian, J., Zhang, R., He, D. & Chen, Q. Study on the relationship between soil emissivity spectra and content of soil element. *Spectrosc Spect Anal.* **37**(02):557-564(2017).
6. Kemper, T. & Sommer, S. Estimate of heavy metal contamination in soils after a mining accident using reflectance spectroscopy. *Environ Sci Technol*. **36**(12), 2742-2747(2002).
7. Panigrahi, N. & Das, B.S. Canopy spectral reflectance as a predictor of soil water potential in rice. *Water Resour Res*. **54**(4), 2544-2560(2018).
8. Peddle, D.R., White, H.P., Soffer, R.J., Miller, J.R. & LeDrew, E.F. Reflectance processing of remote sensing spectroradiometer data. *Computers and Geoences*. **27**(2), 203-213(2001).
9. Ben-Dor, E. *et al*. Using imaging spectroscopy to study soil properties. Remote. Sens. *Environ*. **113**, S38-S55(2009).
10. Rossel, R.A., Walvoort, D.J., Mcbratney, A.B., Janik, L.J. & Skjemstad, J.O. Visible, near infrared, mid infrared or combined diffuse reflectance spectroscopy for simultaneous assessment of various soil properties. *Geoderma*. **131**(1), 59-75(2006).
11. Cheng, H. *et al*. Estimating heavy metal concentrations in suburban soils with reflectance spectroscopy. *Geoderma*. **336**, 59-67(2019).
12. Ding, J., Yang, A., Wang, J., Sagan, V. & Yu, D. Machine-learning-based quantitative estimation of soil organic carbon content by VIS/NIR spectroscopy. *PeerJ*. **6**(3), e5714(2018).
13. Gobrecht, A., Bendoula, R., Roger, J-M. & Bellon-Maurel, V. A new optical method coupling light polarization and vis–NIR spectroscopy to improve the measurement of soil carbon content. *Soil Till Res*. **155**, 461-470(2016).
14. Gu, X., Wang, Y., Song, X. & Xu, X. The inversion model of soil organic matter of cultivated land based on hyperspectral technology. Remote Sensing for Agriculture, Ecosystems, and Hydrology XVII. *International Society for Optics and Photonics*.2015.
15. Nawar, S., Buddenbaum, H., Hill, J., Kozak, J. & Mouazen, A.M. Estimating the soil clay content and organic matter by means of different calibration methods of vis-NIR diffuse reflectance spectroscopy. *Soil Till Res*. **155**, 510-522(2016).

16. Yu, X., Liu, Q., Wang, Y., Liu, X. & Liu, X. Evaluation of MLSR and PLSR for estimating soil element contents using visible/near-infrared spectroscopy in apple orchards on the Jiaodong peninsula. *Catena*. **137**, 340-349(2016).
17. Ji, W.J., Li, X., Li, C.X., Zhou, Y. & Shi, Z. Using different data mining algorithes to predict soil organic matter based on visible-near infrared spectroscopy. *Spectrosc Spect Anal*. **32**(09), 2393-2397(2012).
18. Douglas, R.K., Nawar, S., Alamar, M.C., Mouazen, A.M. & Coulon, F. Rapid prediction of total petroleum hydrocarbons concentration in contaminated soil using vis-NIR spectroscopy and regression techniques. *Sci Total Environ*. **616**, 147-155(2018).
19. Mouazen, A.M. & Al-Asadi, R.A. Influence of soil moisture content on assessment of bulk density with combined frequency domain reflectometry and visible and near infrared spectroscopy under semi field conditions. *Soil Till Res*. **176**, 95-103(2018).
20. Rossel, R.A. & Behrens, T. Using data mining to model and interpret soil diffuse reflectance spectra. *Geoderma.* **158**(1), 46-54(2010).
21. Nawar, S. & Mouazen, A.M. Comparison between random forests, artificial neural networks and gradient boosted machines methods of on-line vis-NIR spectroscopy measurements of soil total nitrogen and total carbon. *Sensors*. **17**(10), 2428(2017).
22. Wang, J., Chen, Y., Chen, F., Shi, T. & Wu, G. Wavelet-based coupling of leaf and canopy reflectance spectra to improve the estimation accuracy of foliar nitrogen concentration. *Agr Forest Meteorol*. **248**, 306-315(2018).
23. Hong, Y. *et al*. Combining fractional order derivative and spectral variable selection for organic matter estimation of homogeneous soil samples by vis–NIR spectroscopy. *Remote Sens.* **10**(3), 479(2018).
24. Sorenson, P.T. *et al*. Monitoring organic carbon, total nitrogen, and pH for reclaimed soils using field reflectance spectroscopy. *Can J Soil Sci.* **97**(2), 241-248(2017).
25. Gomez, C., Rossel, R.A.V. & Mcbratney, A.B. Soil organic carbon prediction by hyperspectral remote sensing and field vis-NIR spectroscopy: An Australian case study. *Geoderma*. **146**(3-4), 403-411(2008).
26. Shi, T.Z. *et al*. Comparison of multivariate methods for estimating soil total nitrogen with visible/near-infrared spectroscopy. *Plant Soil*. **366**(1-2), 363-375(2013).
27. Stenberg, B., Rossel, R.A.V., Mouazen, A.M. & Wetterlind, J. Chapter five-visible and near infrared spectroscopy in soil science. *Adv Agron*. **107**, 163-215(2010).
28. Uddin, M.P., Mamun, M.A. & Hossain, M.A. PCA-based feature reduction for hyperspectral remote sensing image classification. *IETE Tech Rev*. **5**, 1-21(2020).
29. Cambule, A.H., Rossiter, D.G., Stoorvogel, J.J. & Smaling, E.M.A. Building a near infrared spectral library for soil organic carbon estimation in the Limpopo National Park, Mozambique. *Geoderma*. **183**, 41-48(2012).
30. Kawamura, K. *et al*. Vis-NIR spectroscopy and PLS regression with waveband selection for estimating the total C and N of paddy soils in Madagascar. *Remote Sens*. **9**(10), 1081(2017).
31. Leone, A.P., Viscarra-Rossel, R.A., Amenta, P. & Buondonno, A. Prediction of soil properties with PLSR and vis-NIR spectroscopy: Application to mediterranean soils from southern Italy. *Curr Anal Chem*. **8**(2), 283-299(2012).
32. Wang, S., Chen, Y., Wang, M., Zhao, Y. & Li, J. SPA-based methods for the quantitative estimation of the soil salt content in saline-alkali land from field spectroscopy data: A case

study from the Yellow River irrigation regions. *Remote Sens*. **11**(8), 967(2019).
33. Barnes, E.M. *et al*. Remote- and ground-based sensor techniques to map soil properties. Photogramm. *Eng Rem S*. **69**(6), 619-630(2003).
34. Priori, S. *et al*. Field-scale mapping of soil carbon stock with limited sampling by coupling gamma-ray and vis-NIR spectroscopy. *Soil Sci Soc Am J*. **80**(4), 954-964(2016).
35. Amin, I., Fikrat, F., Mammadov, E. & Babayev, M. Soil organic carbon prediction by vis-NIR spectroscopy: Case study the Kur-Aras plain, Azerbaijan. *Commun Soil Sci Plan*. **51**(6), 726-734(2020).
36. Yu, L. *et al*. Hyperspectral estimation of soil organic matter content based on partial least squares regression. *Transactions of the CSAE*. **31**(14), 103-109(2015).
37. Liu, Y.F., Lu, Y.N., Guo, L., Xiao, F.T. & Chen, Y.Y. Construction of calibration set based on the land use types in visible and near-infrared(VIS-NIR)model for soil organic matter estimation. *Acta Pedologica Sinica*. **53**, 332-341(2016).
38. Chen, Y.Y., Qi, K., Liu, Y.L., He, J.H. & Jiang, Q.H. Transferability of hyperspectral model for estimating soil organic matter concerned with soil moisture. *Spectrosc Spect Anal*. **35**(06), 1705-1708(2015).
39. Emmanuelle, V., Zoran, C., Dav, E. & Gwendal, L. Predicting key agronomic soil properties with UV-vis fluorescence measurements combined with Vis-NIR-SWIR reflectance spectroscopy: A farm-scale study in a mediterranean viticultural agroecosystem. *Sensors*. **18**(4), 1157(2018).
40. Lu, P., Wei, Z.Q. & Niu, Z. Estimate of soil attributes using the method of special band and reflectance inflection diffference. *Spectrosc Spect Anal*. **29**(03), 716-721(2009).
41. Zhou, X.M., & Zhang, T. Analysis of the April 2019 atmospheric circulation and weather. *Meteor Mon*. **45**(7), 1028-1036(2019).
42. Guan, L. & Zhang, T. Analysis of the May 2019 atmospheric circulation and weather. *Meteor Mon*. **45**(8), 1181-1188(2019).
43. Li, X., He, Y. & Wu, C. Non-destructive discrimination of paddy seeds of different storage age based on Vis/NIR spectroscopy. *J Stored Prod Res*. **44**(3), 264-268(2008).
44. Boško, M. & Bensa, A. Prediction of soil organic carbon using VIS-NIR spectroscopy: Application to Red Mediterranean soils from Croatia. *Eurasian J Soil Sci*. **6**(4), 365-373(2017).
45. McCarty, G.W., Reeves III, J.B., Reeves, V.B., Follett, R.F. & Kimble, J.M. Mid-infrared and near-infrared diffuse reflectance spectroscopy for soil carbon measurement. *Soil Sci Soc Am J*. **66**(2), 640-646(2002).
46. Gholizadeh, A. *et al*. Comparing different data preprocessing methods for monitoring soil heavy metals based on soil spectral features. *Soil Water Res*. **10**(4), 218-227(2015).
47. Wang, X., Xue, L., He, X.W. & Liu, M.H. Vitamin C content estimation of chilies using Vis/NIR spectroscopy. *International conference on electric information and control engineering*. **2011**, 1894-1897(2011).
48. Lee, K.S. *et al*. Wavelength identification and diffuse reflectance estimation for surface and profile soil properties. *American Society of Agricultural and Biological Engineers.* **52**(3), 683-695(2009).

Acknowledgements:

This work was supported by National Natural Science Foundation of China(31871571, 31371572), Outstanding Doctor Funding Award of Shanxi Province(SXYBKY2018040), Scientific and Technological Innovation Fund of Shanxi Agricultural University(2018YJ17), Applied Basic Research Project of Shanxi Province(201801D221299), and Science and Technique Innovation Project of Shanxi Agricultural University(2020BQ32).

Author Contributions:

Study concept and design: M.C.F., and Y.K.X. Data analysis and drafting of the manuscript: C.B.Y. Experimental participants: L.F.S., B.H.J., Y.K.X., and M.S. Critical revision of the manuscript for important intellectual content: M.C.F., C.W., L.J.X., M.J.Z., and X.Y.S.. Obtained funding: W.D.Y., C.W. and L.J.X. Study supervision: M.C.F.

Additional Information:

Competing Interestes: The authors declare no competing interests.

Figures:

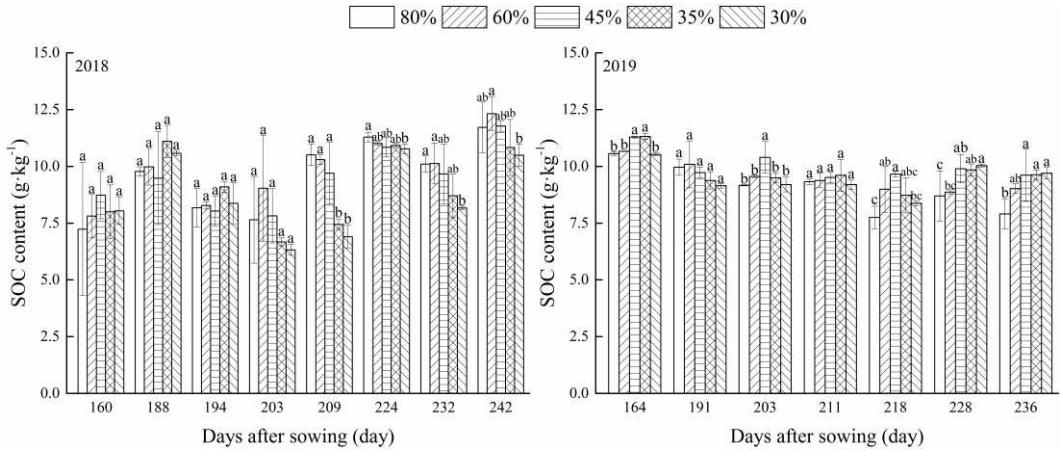

Fig.1. Changes of SOC content under different water treatments

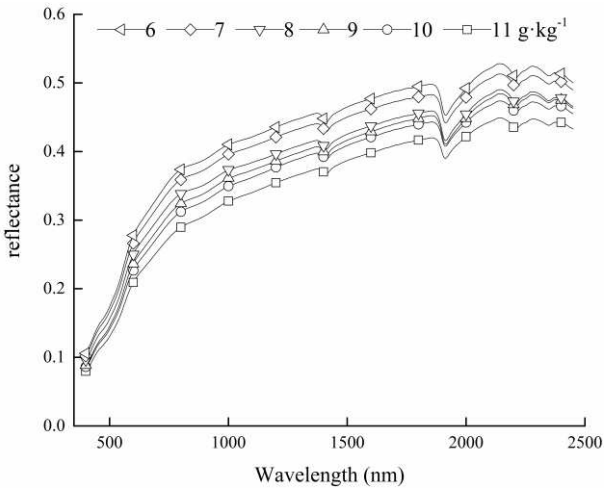

442

443 Fig.2. Spectral reflectance changes of soils with different SOC contents

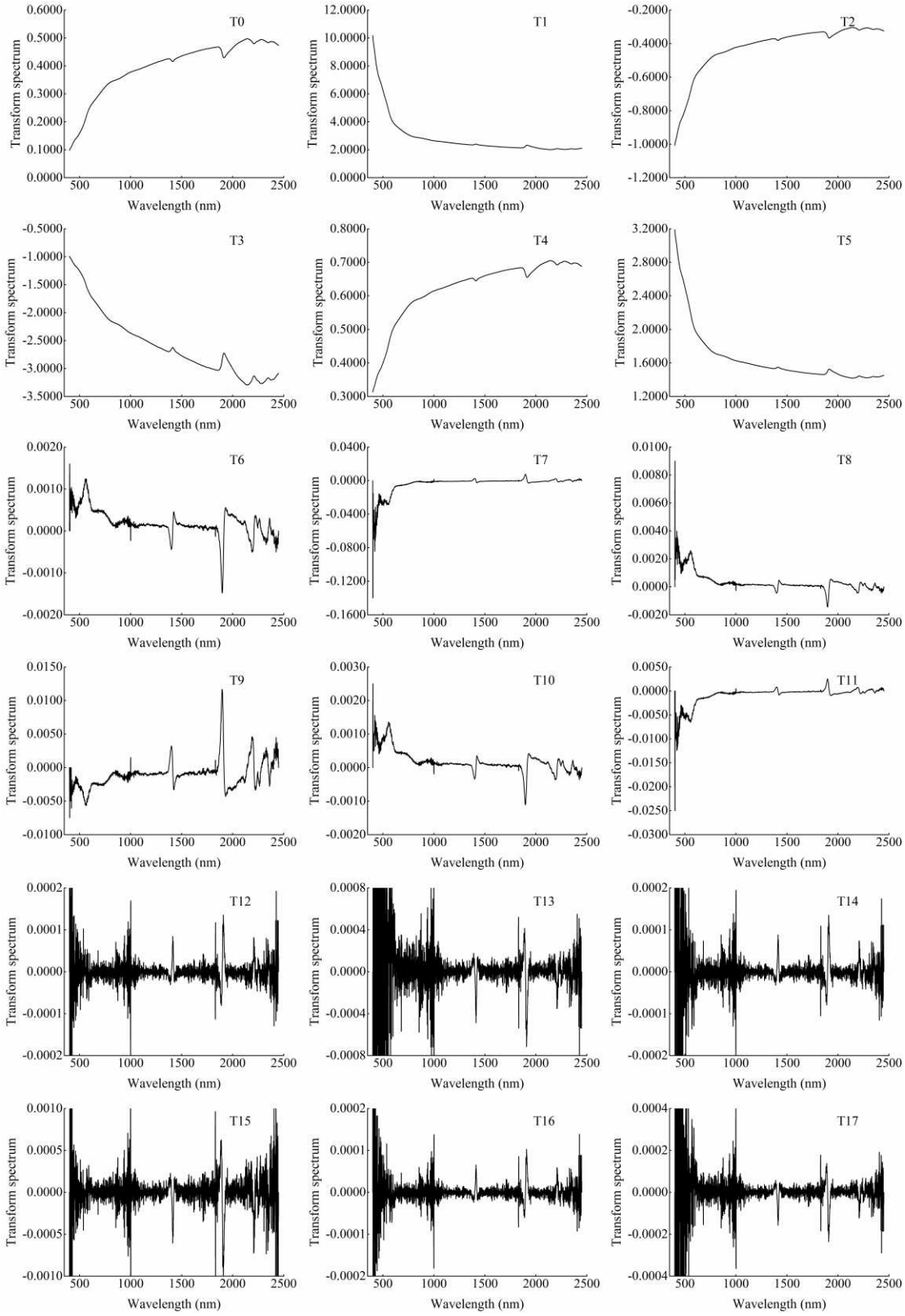

Fig.3. Spectral curves of different preprocessing mathematical algorithms

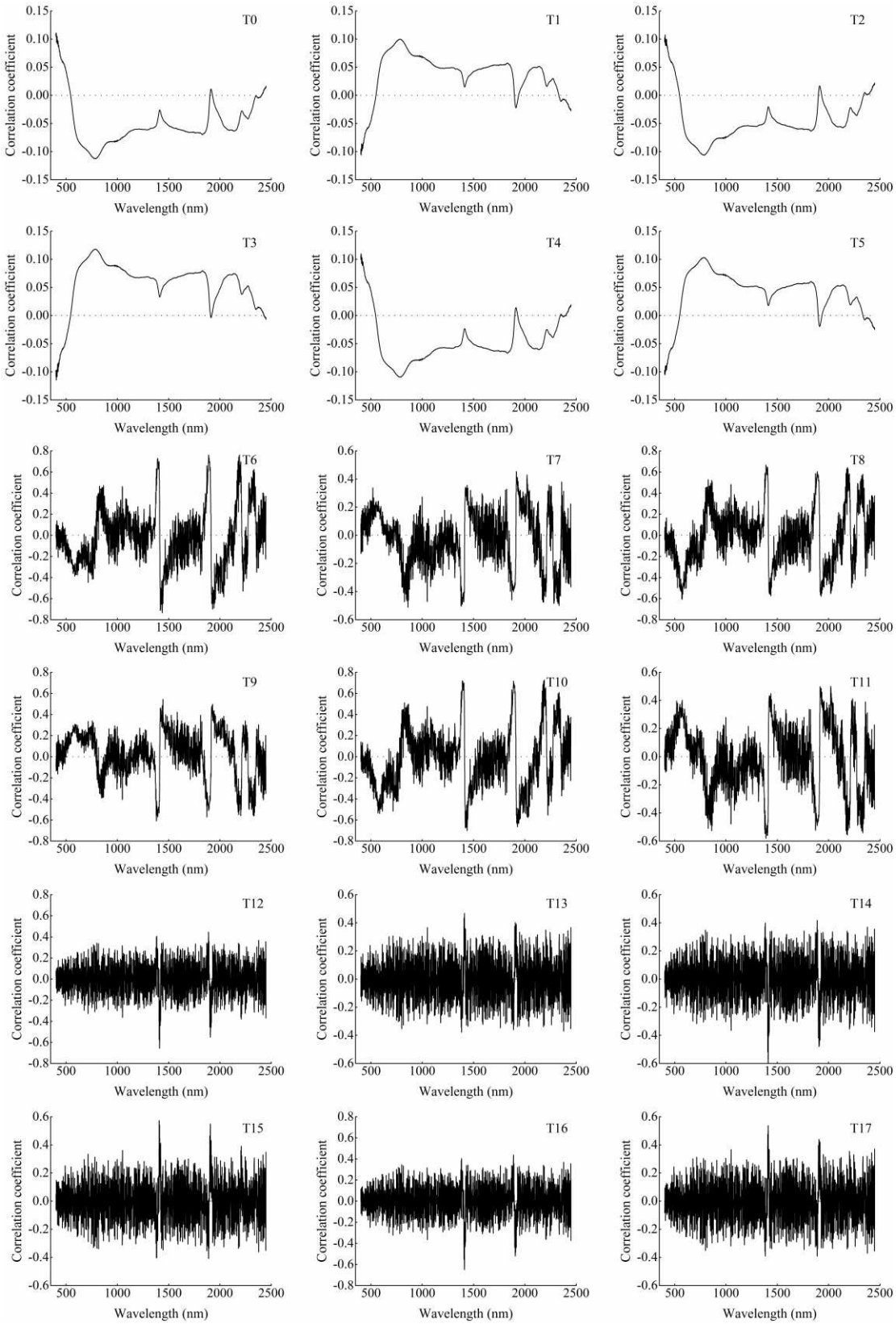

Fig.4. Correlation of different mathematical transformation spectra and SOC content

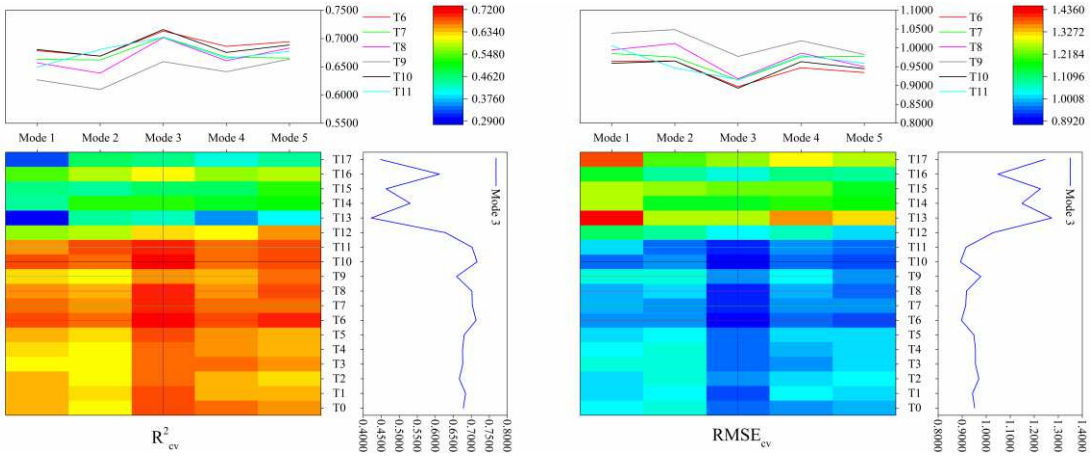

448

449 Fig.5. Construction of PLSR models in different modes

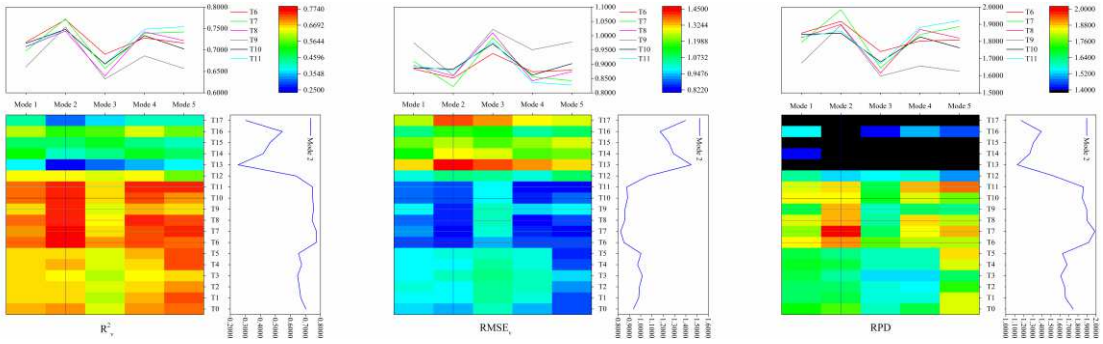

450

451 Fig.6. Validation of PLSR models in different modes

452